PHYSICAL REVIEW A **96**, 041603(R) (2017)

Topological properties of a dense atomic lattice gas

Robert J. Bettles,[1] Jiří Minář,[2,3] Charles S. Adams,[1] Igor Lesanovsky,[2,3] and Beatriz Olmos[2,3,*]

[1]*Joint Quantum Center (JQC) Durham-Newcastle, Department of Physics, Durham University, South Road, Durham DH1 3LE, United Kingdom*

[2]*School of Physics and Astronomy, The University of Nottingham, Nottingham NG7 2RD, United Kingdom*

[3]*Centre for the Mathematics and Theoretical Physics of Quantum Non-Equilibrium Systems, The University of Nottingham, Nottingham NG7 2RD, United Kingdom*

(Received 15 March 2017; revised manuscript received 13 June 2017; published 10 October 2017)

We investigate the existence of topological phases in a dense two-dimensional atomic lattice gas. The coupling of the atoms to the radiation field gives rise to dissipation and a nontrivial coherent long-range exchange interaction whose form goes beyond a simple power law. The far-field terms of the potential—which are particularly relevant for atomic separations comparable to the atomic transition wavelength—can give rise to energy spectra with one-sided divergences in the Brillouin zone. The long-ranged character of the interactions has another important consequence: it can break the standard bulk-boundary relation in topological insulators. We show that topological properties such as the transport of an excitation along the edge of the lattice are robust with respect to the presence of lattice defects and dissipation. The latter is of particular relevance as dissipation and coherent interactions are inevitably connected in our setting.

DOI: 10.1103/PhysRevA.96.041603

Introduction. Recently, the pursuit of topological phases in quantum many-body systems has been the focus of intense research. The potential application of these topological states for robust quantum computation [1,2] is one of the driving forces for this increased interest. So-called topological insulators are usually characterized by bulk bands separated by a gap and the presence of gapless edge states whose properties are topologically protected against local perturbations such as external disorder or noise [3,4]. Paradigmatic examples of these include the integer and fractional quantum Hall effects, which were initially realized on two-dimensional electron gases subject to strong magnetic fields [5–8]. Since their discovery, several lattice models that do not require external magnetic fields have been proposed and some realized experimentally [9–24].

Due to the high degree of experimental control that is achievable nowadays, cold atoms and molecules have been proposed as platforms for the exploration of novel topological phases of quantum matter [25]. In particular, many-body systems that display long-range interactions [26–31]—such as polar molecules [32–36], atoms with large magnetic dipoles [37], and Rydberg atoms [38]—have been shown to feature topologically nontrivial flat bands and fractional quantum Hall states.

In this Rapid Communication, we explore the topological properties of a two-dimensional lattice of atoms where long-range interactions arise intrinsically via coherent light scattering between internal atomic states [39]. We consider the full interaction—going beyond the usually employed near-field approximation—which is of relevance for atomic separations comparable to the atomic transition wavelength. This scenario is currently studied in various contexts, e.g., the exploration of collective light scattering and super- and subradiant decay [39–46]. We study two lattice geometries (a square and a honeycomb lattice) and find that this simple system can support topologically nontrivial phases. The often neglected far-field terms of the interactions lead to one-sided divergences in the single-particle spectrum. We explore the consequences of the long-ranged character of the interaction on the relation between the topological properties of the bulk and the boundary of a finite-size system. We find that the standard bulk-boundary relation [47,48], well established for short-range interactions, does not generally hold [30,31]. Furthermore, we find that neither the presence of lattice defects nor dissipation destroy the topological properties of the system. The latter is of particular importance as the considered system is inevitably open: both dissipation and coherent exchange interactions originate from the coupling of the atoms to the radiation field.

The system. We consider a two-dimensional optical lattice with N sites in the xy plane (lattice spacing a), where each site is occupied by a single atom. The jth atom is located at position $\mathbf{r}_j$ with internal levels $|g\rangle_j$ (ground state) and $|-\rangle_j$, $|0\rangle_j$, $|+\rangle_j$ (excited states) corresponding to the $J=0$ and $J=1$ total angular momentum manifolds, respectively [see Fig. 1(a)]. This level structure is naturally available in a variety of systems such as alkaline-earth-metal atoms [49–51], dysprosium atoms [37], polar molecules [36,52,53], or Rydberg systems [38].

The coupling of the atoms to the quantized multimode radiation field results in an effective long-range exchange interaction and collective dissipation [54–56]. Within the dipole and Born-Markov approximations, the dynamics of the atomic system is described by the master equation

$$\dot{\rho} = -\frac{i}{\hbar}[H,\rho] + \mathcal{D}(\rho), \tag{1}$$

with

$$H = \hbar \sum_{j\neq l} \mathbf{d}_j^\dagger \cdot \overline{V}_{jl} \cdot \mathbf{d}_l, \tag{2}$$

and

$$\mathcal{D}(\rho) = \sum_{jl} \mathbf{d}_j \cdot \overline{\Gamma}_{jl} \cdot \rho \mathbf{d}_l^\dagger - \frac{1}{2}\{\mathbf{d}_j^\dagger \cdot \overline{\Gamma}_{jl} \cdot \mathbf{d}_l, \rho\}. \tag{3}$$

*beatriz.olmos-sanchez@nottingham.ac.uk

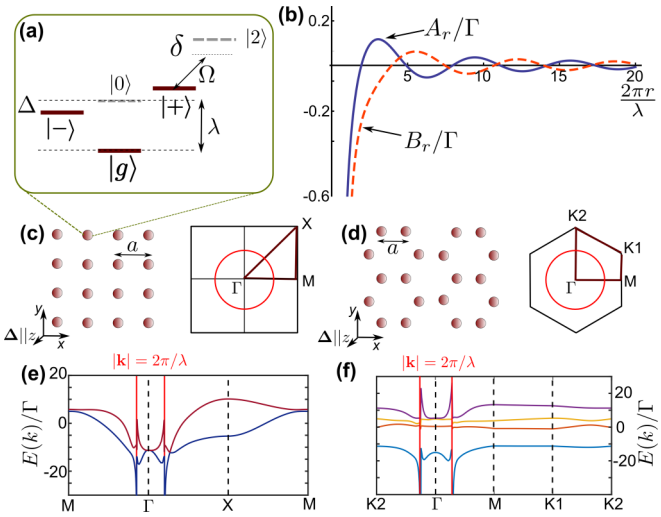

FIG. 1. (a) Internal atomic level structure. Time-reversal symmetry is broken via a magnetic field of strength Δ/μ_B perpendicular to the lattice and the off-resonant coupling of $|+\rangle$ to an auxiliary state $|2\rangle$ with $\varepsilon \approx \Omega/2\delta \ll 1$. (b) Hamiltonian coefficients A_r [Eq. (6), solid line] and B_r [Eq. (7), dashed line] vs r/λ. (c) and (d) Real-space configurations and first Brillouin zone for SL and HL, respectively. The red circle represents the points of divergence and discontinuity of the spectrum for $a/\lambda = 0.1$. (e) and (f) Dispersion relations for the SL and the HL, respectively, which exhibit the existence of a one-sided divergence at $|\mathbf{k}| = 2\pi/\lambda$.

Here, $\mathbf{d}_j = (|g\rangle_j\langle+|, |g\rangle_j\langle-|)^T$ are hard-core boson operators and

$$\overline{V}_{jl} = \begin{pmatrix} A_{jl} & B_{jl}e^{-2i\phi_{jl}} \\ B_{jl}e^{2i\phi_{jl}} & A_{jl} \end{pmatrix}, \tag{4}$$

$$\overline{\Gamma}_{jl} = \begin{pmatrix} A'_{jl} & B'_{jl}e^{-2i\phi_{jl}} \\ B'_{jl}e^{2i\phi_{jl}} & A'_{jl} \end{pmatrix}. \tag{5}$$

Note that here we have used the fact that the dynamics of $|0\rangle$ and the $\{|-\rangle, |+\rangle\}$ manifold are decoupled, further explained in the Supplemental Material [57]. The coefficients in Eqs. (4) and (5) read

$$A_{jl} = \frac{3\Gamma}{8}\left[-\frac{\cos\kappa_{jl}}{\kappa_{jl}} - \frac{\sin\kappa_{jl}}{\kappa_{jl}^2} - \frac{\cos\kappa_{jl}}{\kappa_{jl}^3}\right], \tag{6}$$

$$B_{jl} = \frac{3\Gamma}{8}\left[\frac{\cos\kappa_{jl}}{\kappa_{jl}} - 3\left(\frac{\sin\kappa_{jl}}{\kappa_{jl}^2} + \frac{\cos\kappa_{jl}}{\kappa_{jl}^3}\right)\right], \tag{7}$$

$$A'_{jl} = \frac{3\Gamma}{4}\left[\frac{\sin\kappa_{jl}}{\kappa_{jl}} - \frac{\cos\kappa_{jl}}{\kappa_{jl}^2} + \frac{\sin\kappa_{jl}}{\kappa_{jl}^3}\right], \tag{8}$$

$$B'_{jl} = \frac{3\Gamma}{4}\left[-\frac{\sin\kappa_{jl}}{\kappa_{jl}} - 3\left(\frac{\cos\kappa_{jl}}{\kappa_{jl}^2} - \frac{\sin\kappa_{jl}}{\kappa_{jl}^3}\right)\right], \tag{9}$$

where Γ is the single atom decay rate and $\kappa_{jl} \equiv 2\pi r_{jl}/\lambda$ represents a reduced distance between the jth and lth atom, with λ being the wavelength of the transition from the ground to the excited state manifold [see Fig. 1(a)], $r_{jl} = |\mathbf{r}_j - \mathbf{r}_l|$, and $\phi_{jl} = \arg(\mathbf{r}_j - \mathbf{r}_l)$ is the polar angle between the atoms.

The many-body Hamiltonian (2) conserves the number of excitations in the system and describes their exchange among the atoms. The coefficients in this Hamiltonian [Eqs. (6) and (7)] decay as $1/r^3$ for short distances ($r \leqslant \lambda$) and as $1/r$ for $r \gg \lambda$ [see Fig. 1(b)]. We will study the topological properties of the system in an intermediate regime, where the full potential needs to be considered. In particular, we fix the ratio $a/\lambda = 0.1$ [43,51] (the effects we demonstrate are not constrained to this specific value) and systematically investigate two lattice geometries: the square lattice (SL) and the honeycomb lattice (HL) [see Figs. 1(c) and 1(d), respectively]. We proceed by analyzing first the band structure of the Hamiltonian (2) and then studying the effect of dissipation (3) on the edge transport in the topologically nontrivial phases.

Band structure and divergences. To obtain the band structure we express (2) in the reciprocal space as

$$H = \hbar \sum_{\mathbf{k}} \psi_{\mathbf{k}}^\dagger \cdot \overline{V}_{\mathbf{k}} \cdot \psi_{\mathbf{k}}, \tag{10}$$

where

$$\psi_{\mathbf{k}} = \frac{1}{\sqrt{N}} \sum_l \mathbf{d}_l e^{i\mathbf{k}\cdot\mathbf{r}_l}, \tag{11}$$

and

$$\overline{V}_{\mathbf{k}} = \sum_{\mathbf{r}\neq 0} e^{i\mathbf{k}\cdot\mathbf{r}} \overline{V}_{\mathbf{r}}, \tag{12}$$

with $\mathbf{r}$ being the vector separating any pair of atoms. Note that the potential (14) (due to the terms that decay as $1/r$) makes the sum in Eq. (12) not convergent. Potentials with similar features have been shown to lead to interesting physical effects, such as supersonic spreading of the correlations [15–22,58]. Such potentials are also encountered in self-gravitating systems [59] or in electrons in solids subject to the Coulomb force [60].

To evaluate the sum (12) we employ the Ewald summation technique [57,60,61]. As a result, we find that $\overline{V}_{\mathbf{k}}$ features one-sided divergences in the ground state of the spectrum occurring for wave vectors lying on a circle of radius $\kappa = 2\pi/\lambda$ in reciprocal space. More specifically, the potential diverges as $\lim_{k\to\kappa^+}\langle\overline{V}_{\mathbf{k}}\rangle = -\infty$, while $\lim_{k\to\kappa^-}\langle\overline{V}_{\mathbf{k}}\rangle$ remains finite. This situation is depicted in Figs. 1(e) (SL) and 1(f) (HL). In this work we only study cases where the divergence falls inside the Brillouin zone, $a/\lambda < 1/2$ for SL and $a/\lambda < 1/3$ for HL.

Note that in the derivation of the master equation (1) the finite propagation time of the radiation modes mediating the exchange of photons in the system is neglected, i.e., the interaction is considered to be instantaneous [54,62,63]. While this is typically a valid approximation for a finite system, when calculating the band structure the potential is considered in the thermodynamic limit, a situation that is ill-defined and which leads to the appearance of the unphysical divergences and nonanalyticities in the spectrum.

Chern numbers. In the language of differential geometry, the topological properties are studied in terms of differentiable fiber bundles assuming a differentiable Hamiltonian map $H : T^2 \to \mathcal{M}$, mapping the Brillouin zone (represented as a two-dimensional torus T^2) to some target space $\mathcal{M}$ [64]. Here the

topology is characterized by the Chern number defined as

$$C = \frac{1}{2\pi i}\int_{T^2} d\mathbf{k}\, F_{xy}(\mathbf{k}), \tag{13}$$

where $F_{xy}(\mathbf{k}) = \partial_x A_y(\mathbf{k}) - \partial_y A_x(\mathbf{k})$, $A_\mu(\mathbf{k}) = \langle n(\mathbf{k})|\partial_\mu|n(\mathbf{k})\rangle$ is the Berry connection, $|n(\mathbf{k})\rangle$ is an eigenstate of the Hamiltonian (10), $\partial_\mu = \partial/\partial k_\mu$, $\mu = \{x, y\}$, and $\mathbf{k} \in T^2$.

In the present case the assumption of differentiability is in principle not satisfied due to the discontinuity of $\overline{V}_{\mathbf{k}}$. However, formally it is still possible to evaluate the Chern number using the algorithm of Ref. [65], where one avoids the points in the Brillouin zone where $\overline{V}_{\mathbf{k}}$ diverges. This corresponds to evaluating (13) with an effectively bounded Hamiltonian, which in turn yields integer values of C.

Hamiltonian (2) is invariant under time-reversal symmetry (TRS), generated by $\mathcal{T} = \sigma_x\mathcal{K}$, where σ_x is the Pauli matrix and $\mathcal{K}$ the conjugation operator. It has been shown that for such Hamiltonian, at least in the near-field limit where the interactions can be considered short-ranged, breaking TRS is a necessary condition to achieve topologically nontrivial phases in two dimensions [36,66–70]. This can be achieved by lifting the degeneracy of the states $|\pm\rangle$ by means of a uniform magnetic field of strength Δ/μ_B [see Fig. 1(a)]. Alternatively, one can couple the state $|+\rangle$ via a microwave field to an auxiliary hyperfine state, $|2\rangle$ [36]. Assuming this coupling to be off-resonant, such that the detuning of the microwave field, δ, is much larger than its Rabi frequency Ω, the state $|2\rangle$ can be adiabatically eliminated. Defining $\varepsilon = \Omega/2\delta \ll 1$, the effective potential (4) becomes, up to the second order in ε,

$$\overline{V}_{jl} = \begin{pmatrix} (A_{jl} + \Delta\delta_{jl})(1-\varepsilon^2) & B_{jl}e^{-2i\phi_{jl}}\left(1-\frac{\varepsilon^2}{2}\right) \\ B_{jl}e^{2i\phi_{jl}}\left(1-\frac{\varepsilon^2}{2}\right) & A_{jl} - \Delta\delta_{jl} \end{pmatrix}, \tag{14}$$

where δ_{jl} is the Kronecker delta symbol.

After calculating the Chern number of each band for a range of TRS-breaking parameters, the resulting phase diagrams are shown in Figs. 2(a) (SL) and 2(b) (HL). We note that in the SL case it is required that $\varepsilon \neq 0$ in order to access the topologically nontrivial region (nonzero Chern numbers), while in HL several topologically distinct regions can be accessed by tuning Δ alone (i.e., $\varepsilon = 0$). Here, each change in the Chern number is related to the closing of the bulk gap (see [57] for the discussion of the finite-size effects).

Edge states. A hallmark of the nontrivial topology of the bulk is the appearance of edge states. They can be identified by considering an infinite strip keeping the system finite in the y direction, such that the edge states appear as gapless states that cross the gaps between the bands formed by bulk states [see Figs. 2(c) (SL) and 2(d) (HL) for a fixed value of the TRS-breaking parameters]. It is easy to verify that in the example shown, indeed the Hall conductivity or, equivalently, the sum of the Chern numbers of the filled bands below a band gap, determines the net number of edge states crossing that gap (bulk-edge correspondence) [47,48,72]. Note that in the SL the edge states are nearly degenerate and "energetically hidden" [36,69] making it difficult to access them experimentally. However, in the HL relatively well separated bands form, which motivates us to focus on the HL.

One important consequence of the long-ranged character of the interactions in the context of topological systems is that the bulk-edge correspondence, well established for systems with short-range potentials does not necessarily hold (see [31] in the context of one-dimensional free fermions). In the present case we interpret this breaking of the bulk-edge correspondence in terms of the overlap of the edge modes with the bulk [57]. We discuss a specific manifestation of this phenomenon in the form of inhibited excitation propagation along the edge of a finite system in the next section.

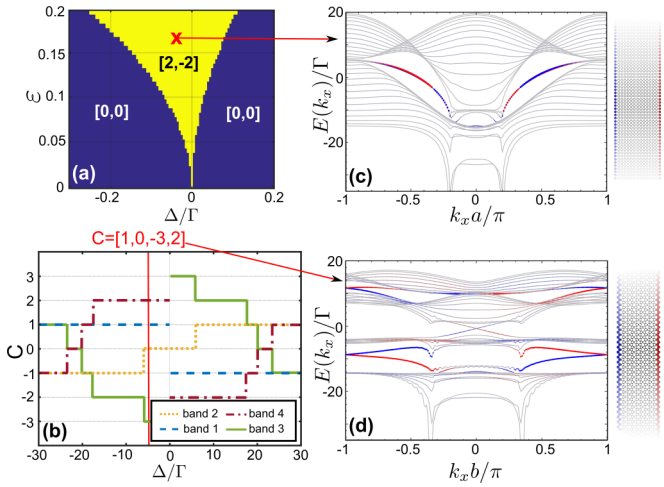

FIG. 2. (a) Phase diagram in the Δ-ε plane for the SL. (b) Phase diagram as a function of Δ for the HL. The numbers in the square brackets indicate the Chern numbers and are ordered from the lowest to highest energy bands. (c) and (d) Spectrum in the infinite strip geometry for the SL [$N_y = 15$ atoms, $\varepsilon = 0.17$, $\Delta/\Gamma = -0.05$, red cross in (a)] and HL [$N_y = 20$ atoms, $\Delta/\Gamma = -5$, bearded zigzag boundary conditions [71], red line in (b)]. Note that with these boundary conditions $b = \sqrt{3}a$ denotes the spacing between neighboring unit lattice sites in the y direction. The size of the points indicate the weight of the given eigenmode on one (red) or the other (blue) edge of the strip (schematically shown on the right).

Finite system: Quasimomentum and driven-dissipative dynamics. In a finite system, to obtain a measure of whether any given mode has a chiral edge conductivity associated with it, we define a *quasimomentum* following a similar approach to [69,73]. When an excitation hops from site to site, it accumulates a phase. If this phase is constant around the edge of the lattice, the hopping occurs in a given direction. If the hopping phase is random between different lattice sites, however, there is no preferred direction of hopping. We therefore define the *quasimomentum*, q, as the average phase difference between neighboring lattice sites:

$$q = \frac{1}{N_{\text{edge}}}\text{Im}\left[\ln\sum_{l=1}^{N_{\text{edge}}}\frac{\mathbf{d}_l^\dagger\mathbf{d}_{l+1}}{|\mathbf{d}_l^\dagger\mathbf{d}_{l+1}|}\right], \tag{15}$$

where N_{edge} is the number of atoms in the outermost edge of the lattice. In Fig. 3(a) we show the quasimomentum spectrum for a HL of hexagonal shape with a total of 486 atoms. We have overlaid the band structure results for an infinite strip with the same number of atoms in the y direction ($N_y = 20$) for comparison.

Another defining characteristic of an edge state is that most of its weight is on the physical edge of the system. Writing

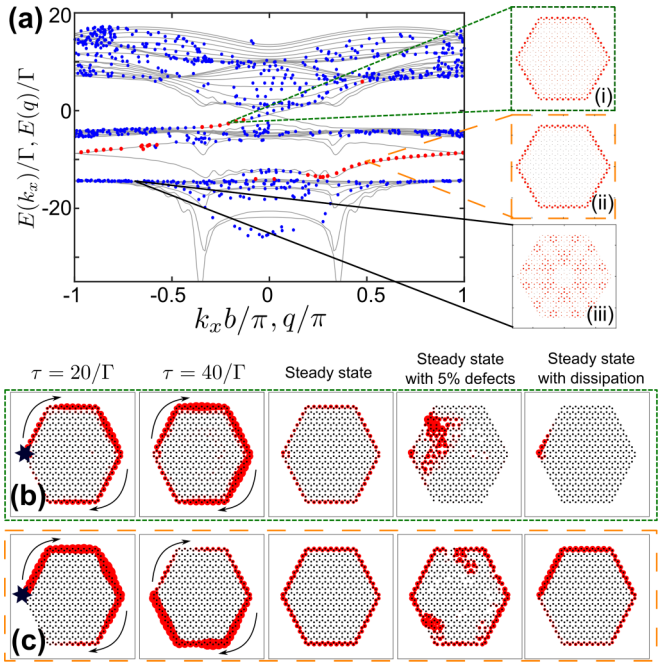

FIG. 3. (a) Energy vs quasimomentum of a finite HL of hexagonal shape with the total of 486 sites (dots) together with the spectrum of the infinite strip geometry [gray lines, same parameters as in Fig. 2(d)]. The blue (red) dots represent states with less (more) than 95% spatial support on the edge of the lattice (see text for details). (i)–(iii) show the spatial configuration of the indicated eigenstates. (b) and (c) show the excitation dynamics (direction of travel given by the arrows) and the steady state (with defects and dissipation) under the driving of a single atom on the edge (indicated by the star in the leftmost panels) with detuning -2Γ and -10Γ, respectively.

an eigenstate of the system as $|\varphi\rangle = \sum_{\mu,j} c_\mu^j |\mu\rangle_j$, where $\mu \in \{-,+\}$ and j index the internal degrees of freedom and the spatial position, respectively, we quantify the weight of the eigenstate on the edge of the system as $w = \sum_{\mu,j\in\text{edge}} |c_\mu^j|^2$. The blue and red dots in Fig. 3(a) correspond to states where $w < 0.95$ and $w > 0.95$, respectively. The spatial distributions of the excitation in two eigenstates located in the middle and lowest gaps are shown in Figs. 3(i) and 3(ii) [which we denote as states (i) and (ii) in the following]. An eigenstate in the bulk is shown for comparison in Fig. 3(iii). The size of the red circles corresponds to the probability of excitation at a given site.

In order to further characterize the edge states in the finite system, we model the dynamics of an excitation in the lattice under the Hamiltonian (2). Specifically, we drive a single atom on the leftmost corner of the HL [marked by a star in the leftmost panels of Figs. 3(b) and 3(c)] with weak driving strength and σ_- polarization. We fix the detuning to -2Γ and -10Γ [Figs. 3(b) and 3(c), respectively], so that we resonantly address the states (i) and (ii), respectively. In the first two panels, snapshots of the propagation at $\tau = 20\Gamma$ and 40Γ, we observe that in both states the excitation dynamics is chiral with clockwise propagation. The third panel shows the excitation in the steady state.

One of the features of the edge states is their robustness against local perturbations. In order to probe this, next we simulate the excitation dynamics including 5% of uniformly distributed lattice defects, i.e., empty sites due to an imperfect loading of atoms [fourth panels in Figs. 3(b) and 3(c)]. We observe a clear difference in the excitation propagation when driving the state (i), where the propagation is clearly interrupted, and the state (ii), where the excitations still populate a significant part of the edge. This strongly indicates that only state (ii) is a topological edge state [57]. The behavior persists independently of the state one chooses to address in both gaps. This is in contrast to what one might expect from the equilibrium bulk analysis, where the edge state conductivity, proportional to the sum of the Chern numbers of the filled lower lying bands, is the same for both states (i) and (ii).

Finally, as the mechanism that is responsible for the existence of coherent interactions is also responsible for the dissipation in the system, we simulate the dynamics above including the dissipative term (3). As was shown in [74] and also observed in [75], all states that lie outside the circle $|\mathbf{k}| = \kappa$ are subradiant, i.e., they decay with a rate much smaller than the single atom decay rate Γ. Hence, remarkably, we find that while in case (i) the dissipation makes the excitation decay after only a few sites, the excitation in case (ii) is much less affected by the dissipation (see discussion in [57]).

Experimental considerations. One of the main attractive features of this system is the relative experimental simplicity of the setup. A lattice gas of alkaline-earth-metal atoms such as strontium [51,76] or ytterbium [77] represents a promising platform for the realization of the present scheme. For example, in bosonic strontium the transition between the triplet states $^3P_0$-$^3D_1$ has an associated wavelength $\lambda = 2.6\ \mu$m. It was shown in [51] that these atoms can be trapped in an optical lattice with $\lambda_{\text{latt}} = 412.8$ nm, entailing $a/\lambda \approx 0.08$ (SL) and 0.03 (HL). Another alternative for the creation of such subwavelength lattices is based on photonic crystal waveguides [78]. Finally, the detection of these topological phases could be achieved via light scattering of a weak laser field from the lattice [79–82].

Conclusions and outlook. We have found the existence of topologically nontrivial phases in a dense atomic two-dimensional lattice system coupled to the radiation field. We have shown that one can excite edge states that allow for the transport of an excitation over long distances along the edge of the lattice that are robust to the presence of defects. Moreover, these edge states are remarkably long-lived due to the collective character of the dissipation (this effect has also been investigated in [74,75]). Finally, we have found that, due to the long-ranged character of the interactions, the bulk-boundary relations, well established for topological insulators with short-range interactions, are not generally valid in our setting.

Acknowledgments. The authors thank M. Marcuzzi, S. Powell, and S. Weber, and R.J.B. thanks J. Perczel and D. S. Wild for useful discussions. The research leading to these results has received funding from the European Research Council under the European Union's Seventh Framework Programme (FP/2007-2013)/ERC Grant Agreement No. 335266 (ESCQUMA) and the EPSRC Grant No. EP/M014266/1. R.J.B. acknowledges funding from the UK EPSRC (Grant No. EP/L023024/1). B.O. was supported by the Royal Society and EPSRC Grant No. DH130145. C.S.A. also acknowledges support from FET-PROACT project RySQ (H2020-FETPROACT-2014-640378-RYSQ).

[1] A. Kitaev, Ann. Phys. (NY) **303**, 2 (2003).
[2] C. Nayak, S. H. Simon, A. Stern, M. Freedman, and S. Das Sarma, Rev. Mod. Phys. **80**, 1083 (2008).
[3] M. Z. Hasan and C. L. Kane, Rev. Mod. Phys. **82**, 3045 (2010).
[4] N. Yao, C. Laumann, A. Gorshkov, H. Weimer, L. Jiang, J. Cirac, P. Zoller, and M. Lukin, Nat. Commun. **4**, 1585 (2013).
[5] K. v. Klitzing, G. Dorda, and M. Pepper, Phys. Rev. Lett. **45**, 494 (1980).
[6] R. B. Laughlin, Phys. Rev. B **23**, 5632 (1981).
[7] D. C. Tsui, H. L. Stormer, and A. C. Gossard, Phys. Rev. Lett. **48**, 1559 (1982).
[8] R. B. Laughlin, Phys. Rev. Lett. **50**, 1395 (1983).
[9] F. D. M. Haldane, Phys. Rev. Lett. **61**, 2015 (1988).
[10] J. Ruostekoski, G. V. Dunne, and J. Javanainen, Phys. Rev. Lett. **88**, 180401 (2002).
[11] C. L. Kane and E. J. Mele, Phys. Rev. Lett. **95**, 226801 (2005).
[12] K. S. Novoselov, Z. Jiang, Y. Zhang, S. V. Morozov, H. L. Stormer, U. Zeitler, J. C. Maan, G. S. Boebinger, P. Kim, and A. K. Geim, Science **315**, 1379 (2007).
[13] A. Tsukazaki, A. Ohtomo, T. Kita, Y. Ohno, H. Ohno, and M. Kawasaki, Science **315**, 1388 (2007).
[14] M. König, S. Wiedmann, C. Brne, A. Roth, H. Buhmann, L. W. Molenkamp, X.-L. Qi, and S.-C. Zhang, Science **318**, 766 (2007).
[15] S. Raghu, X.-L. Qi, C. Honerkamp, and S.-C. Zhang, Phys. Rev. Lett. **100**, 156401 (2008).
[16] T. Neupert, L. Santos, C. Chamon, and C. Mudry, Phys. Rev. Lett. **106**, 236804 (2011).
[17] Y.-F. Wang, Z.-C. Gu, C.-D. Gong, and D. N. Sheng, Phys. Rev. Lett. **107**, 146803 (2011).
[18] E. Tang, J.-W. Mei, and X.-G. Wen, Phys. Rev. Lett. **106**, 236802 (2011).
[19] K. Sun, Z. Gu, H. Katsura, and S. Das Sarma, Phys. Rev. Lett. **106**, 236803 (2011).
[20] Y.-F. Wang, H. Yao, C.-D. Gong, and D. N. Sheng, Phys. Rev. B **86**, 201101 (2012).
[21] A. Dauphin, M. Müller, and M. A. Martin-Delgado, Phys. Rev. A **86**, 053618 (2012).
[22] N. R. Cooper and J. Dalibard, Phys. Rev. Lett. **110**, 185301 (2013).
[23] M. Barkeshli, N. Y. Yao, and C. R. Laumann, Phys. Rev. Lett. **115**, 026802 (2015).
[24] T. Andrijauskas, E. Anisimovas, M. Račiūnas, A. Mekys, V. Kudriašov, I. B. Spielman, and G. Juzeliūnas, Phys. Rev. A **92**, 033617 (2015).
[25] N. Goldman, J. C. Budich, and P. Zoller, Nat. Phys. **12**, 639 (2016).
[26] Y. Zhang, E. H. Rezayi, and K. Yang, Phys. Rev. B **90**, 165102 (2014).
[27] D. Vodola, L. Lepori, E. Ercolessi, A. V. Gorshkov, and G. Pupillo, Phys. Rev. Lett. **113**, 156402 (2014).
[28] Z.-X. Gong, M. F. Maghrebi, A. Hu, M. L. Wall, M. Foss-Feig, and A. V. Gorshkov, Phys. Rev. B **93**, 041102 (2016).
[29] J. Behrmann, Z. Liu, and E. J. Bergholtz, Phys. Rev. Lett. **116**, 216802 (2016).
[30] O. Viyuela, D. Vodola, G. Pupillo, and M. A. Martin-Delgado, Phys. Rev. B **94**, 125121 (2016).
[31] L. Lepori and L. Dell'Anna, New J. Phys. (to be published), arXiv:1612.08155.
[32] D. Peter, S. Müller, S. Wessel, and H. P. Büchler, Phys. Rev. Lett. **109**, 025303 (2012).
[33] N. Y. Yao, C. R. Laumann, A. V. Gorshkov, S. D. Bennett, E. Demler, P. Zoller, and M. D. Lukin, Phys. Rev. Lett. **109**, 266804 (2012).
[34] S. R. Manmana, E. M. Stoudenmire, K. R. A. Hazzard, A. M. Rey, and A. V. Gorshkov, Phys. Rev. B **87**, 081106 (2013).
[35] N. Y. Yao, A. V. Gorshkov, C. R. Laumann, A. M. Läuchli, J. Ye, and M. D. Lukin, Phys. Rev. Lett. **110**, 185302 (2013).
[36] D. Peter, N. Y. Yao, N. Lang, S. D. Huber, M. D. Lukin, and H. P. Büchler, Phys. Rev. A **91**, 053617 (2015).
[37] N. Y. Yao, S. D. Bennett, C. R. Laumann, B. L. Lev, and A. V. Gorshkov, Phys. Rev. A **92**, 033609 (2015).
[38] M. F. Maghrebi, N. Y. Yao, M. Hafezi, T. Pohl, O. Firstenberg, and A. V. Gorshkov, Phys. Rev. A **91**, 033838 (2015).
[39] R. J. Bettles, S. A. Gardiner, and C. S. Adams, Phys. Rev. A **92**, 063822 (2015).
[40] A. A. Svidzinsky, J.-T. Chang, and M. O. Scully, Phys. Rev. A **81**, 053821 (2010).
[41] J. Keaveney, A. Sargsyan, U. Krohn, I. G. Hughes, D. Sarkisyan, and C. S. Adams, Phys. Rev. Lett. **108**, 173601 (2012).
[42] T. Bienaimé, R. Bachelard, N. Piovella, and R. Kaiser, Fortschr. Phys. **61**, 377 (2013).
[43] J. Pellegrino, R. Bourgain, S. Jennewein, Y. R. P. Sortais, A. Browaeys, S. D. Jenkins, and J. Ruostekoski, Phys. Rev. Lett. **113**, 133602 (2014).
[44] C. C. Kwong, T. Yang, M. S. Pramod, K. Pandey, D. Delande, R. Pierrat, and D. Wilkowski, Phys. Rev. Lett. **113**, 223601 (2014).
[45] S. L. Bromley, B. Zhu, M. Bishof, X. Zhang, T. Bothwell, J. Schachenmayer, T. L. Nicholson, R. Kaiser, S. F. Yelin, M. D. Lukin, A. M. Rey, and J. Ye, Nat. Commun. **7**, 11039 (2016).
[46] S. D. Jenkins, J. Ruostekoski, J. Javanainen, R. Bourgain, S. Jennewein, Y. R. P. Sortais, and A. Browaeys, Phys. Rev. Lett. **116**, 183601 (2016).
[47] Y. Hatsugai, Phys. Rev. Lett. **71**, 3697 (1993).
[48] Y. Hatsugai, Phys. Rev. B **48**, 11851 (1993).
[49] A. V. Gorshkov, A. M. Rey, A. J. Daley, M. M. Boyd, J. Ye, P. Zoller, and M. D. Lukin, Phys. Rev. Lett. **102**, 110503 (2009).
[50] A. V. Gorshkov, M. Hermele, V. Gurarie, C. Xu, P. S. Julienne, J. Ye, P. Zoller, E. Demler, M. D. Lukin, and A. M. Rey, Nat. Phys. **6**, 289 (2010).
[51] B. Olmos, D. Yu, Y. Singh, F. Schreck, K. Bongs, and I. Lesanovsky, Phys. Rev. Lett. **110**, 143602 (2013).
[52] A. V. Gorshkov, K. R. Hazzard, and A. M. Rey, Mol. Phys. **111**, 1908 (2013).
[53] S. V. Syzranov, M. L. Wall, V. Gurarie, and A. M. Rey, Nat. Commun. **5**, 5391 (2014).
[54] R. H. Lehmberg, Phys. Rev. A **2**, 883 (1970).
[55] G. S. Agarwal, Phys. Rev. A **2**, 2038 (1970).
[56] D. F. V. James, Phys. Rev. A **47**, 1336 (1993).
[57] See Supplemental Material at http://link.aps.org/supplemental/10.1103/PhysRevA.96.041603 for details of the derivation of the master equation, the Ewald summation and the impact of the finite-size of the system on its topological properties.
[58] D.-M. Storch, M. Van den Worm, and M. Kastner, New J. Phys. **17**, 063021 (2015).
[59] *Physics of Long-Range Interacting Systems*, edited by A. Campa, T. Dauxois, D. Fanelli, and S. Ruffo (Oxford University Press, Oxford, 2014).

[60] L. Kantorovich, *Quantum Theory of the Solid State: An Introduction* (Springer Science & Business Media, Berlin, 2004), Vol. 136.
[61] L. Bonsall and A. A. Maradudin, Phys. Rev. B **15**, 1959 (1977).
[62] P. W. Milonni and P. L. Knight, Phys. Rev. A **10**, 1096 (1974).
[63] T. Shi, D. E. Chang, and J. I. Cirac, Phys. Rev. A **92**, 053834 (2015).
[64] *Geometry, Topology and Physics*, edited by M. Nakahara (Taylor & Francis, London, 2003).
[65] T. Fukui, Y. Hatsugai, and H. Suzuki, J. Phys. Soc. Jpn. **74**, 1674 (2005).
[66] A. P. Schnyder, S. Ryu, A. Furusaki, and A. W. W. Ludwig, Phys. Rev. B **78**, 195125 (2008).
[67] A. Kitaev, AIP Conf. Proc. **1134**, 22 (2009).
[68] S. Ryu, A. P. Schnyder, A. Furusaki, and A. W. W. Ludwig, New J. Phys. **12**, 065010 (2010).
[69] S. Weber, Master's thesis, University of Stuttgart, Germany (2015).
[70] D. Peter, Ph.D. thesis, University of Stuttgart, Germany (2015).
[71] L. Wang, R.-Y. Zhang, M. Xiao, D. Han, C. T. Chan, and W. Wen, New J. Phys. **18**, 103029 (2016).
[72] R. Liu, W.-C. Chen, Y.-F. Wang, and C.-D. Gong, J. Phys.: Condens. Matter **24**, 305602 (2012).
[73] M. Hafezi, S. Mittal, J. Fan, A. Migdall, and J. M. Taylor, Nat. Photonics **7**, 1001 (2013).
[74] A. Asenjo-Garcia, M. Moreno-Cardoner, A. Albrecht, H. J. Kimble, and D. E. Chang, Phys. Rev. X **7**, 031024 (2017).
[75] J. Perczel, J. Borregaard, D. E. Chang, H. Pichler, S. F. Yelin, P. Zoller, and M. D. Lukin, Phys. Rev. Lett. **119**, 023603 (2017).
[76] S. V. Syzranov, M. L. Wall, V. Gurarie, and A. M. Rey, Nat. Commun. **7**, 13543 (2016).
[77] T. Fukuhara, S. Sugawa, M. Sugimoto, S. Taie, and Y. Takahashi, Phys. Rev. A **79**, 041604 (2009).
[78] A. Gonzlez-Tudela, C.-L. Hung, D. E. Chang, J. I. Cirac, and H. J. Kimble, Nat. Photonics **9**, 320 (2015).
[79] S. D. Jenkins and J. Ruostekoski, Phys. Rev. A **86**, 031602 (2012).
[80] R. J. Bettles, S. A. Gardiner, and C. S. Adams, Phys. Rev. Lett. **116**, 103602 (2016).
[81] G. Facchinetti, S. D. Jenkins, and J. Ruostekoski, Phys. Rev. Lett. **117**, 243601 (2016).
[82] E. Shahmoon, D. S. Wild, M. D. Lukin, and S. F. Yelin, Phys. Rev. Lett. **118**, 113601 (2017).